



FERMILAB-Pub-84/123-T
September, 1984

Finite Volume Effects on Spectrum Calculations: Monte Carlo
Study of an Exactly Solvable Lattice Field Theory[†]

David Hochberg*

The Enrico Fermi Institute and the Department of Physics
The University of Chicago, Chicago, IL 60637

and

H. B. Thacker

Fermi National Accelerator Laboratory
P. O. Box 500, Batavia, IL 60510

[†] Work supported in part by the U.S. Department of Energy under Contract DE-AC02-82ER-40073.

* Address after 1 October 1984: Rutherford Appleton Laboratory, Chilton, Didcot, Oxfordshire OX11 0QX, U. K.

I. Introduction

The formulation of field theory on a lattice has provided a great deal of new insight into both the theoretical and the computational aspects of quantum field theory. Recent large scale Monte Carlo simulations of lattice QCD have produced encouraging results for a variety of hadron properties.¹ Such computer simulations of lattice field theory necessarily entail two limits which must be taken in order to compare with experimental results. One limit involves taking the lattice spacing to zero to recover the results of the continuum theory. In this process, coupling constants and masses must be renormalized as the lattice spacing is taken to zero in order to hold the physical length scale fixed. The other limit, which is of less fundamental conceptual importance but may be equally important as a source of numerical uncertainty,² is the infinite volume limit. Since the limitations of computer speed and available memory tend to restrict the physical size of the lattice to be not much more than the size of a hadron, it is important to understand the effects of a finite lattice volume on the results of numerical calculations.

In this paper we will address the question of finite volume effects by reporting some results of a Monte Carlo study of the Baxter model,³ which is an exactly solvable lattice version of the massive Thirring/sine-Gordon field theory.⁴⁻⁵ This model has an interesting and nontrivial spectrum consisting of both fermions and bosons.⁶ Here we will use the Thirring model interpretation of the spectrum in which the fermions are elementary and the bosons are fermion-antifermion bound states. (In the sine-Gordon interpretation, the fermion is a

topological soliton and the lowest mass boson is elementary.⁷⁾ The Baxter model is only one of many possible lattice formulations of the theory, but it has a number of unique advantages for our purposes. First, the Baxter model action is given exactly in terms of local two-spin and four-spin couplings which become the quadratic and quartic fermion terms of the Thirring model after fermionization. The ability to formulate the Monte Carlo algorithm in terms of spins instead of fermionic variables obviates the usual problems associated with simulation of dynamical fermions. The Baxter formulation incorporates the fermions on the lattice in an exact way, including closed loop effects, and there is thus no uncertainty analogous to that of the quenched approximation in QCD. In addition, for an infinite volume lattice, the Baxter model is itself exactly solvable for arbitrary values of the lattice spacing (i.e. not just in the scaling limit). The finite lattice spacing analogue of the well-known Dashen-Hasslacher-Neveu⁸⁾ bound state spectrum, as well as the fermion mass itself, are given exactly in terms of elliptic functions.⁶⁾ Thus, any measured deviation in the calculated spectrum compared to the analytic results will be strictly attributable to finite size effects. In addition to the lattice size, the Baxter model contains three adjustable parameters.⁹⁾ One of these, Baxter's v parameter, which is associated with the horizontal-vertical asymmetry of the lattice, will be held fixed at the symmetric point $v=0$ throughout this study. The other two parameters correspond to the mass and coupling constant of the Thirring model. One of the nice features of this model is the ability to adjust the coupling constant at will. This allows us to independently vary the size of the bound state wave function and the

size of the lattice while holding the theoretical (i.e. infinite volume) bound state mass fixed and convincingly demonstrate that the finite size effects on the bound state mass are controlled by the relation between these two sizes.

This paper is organized as follows. In Sec. 2 the definition of the massive Thirring model is given and some of the drawbacks of using one of the standard lattice fermion formulations of the model are discussed. We then review the Baxter model and its relation to the massive Thirring model. In Sec. 3 we gather the basic mass formulae relevant to our analysis. The results of the Monte Carlo calculations are presented in Sec. 4. Some conclusions and discussion are given in Sec. 5.

II. The Massive Thirring Model and the Baxter Model

The massive Thirring model is the theory of a self-coupled fermion field in 1+1 dimensions with dynamics determined by the Lagrangian density

$$L = \bar{\psi}(i\partial - m_0)\psi - \frac{1}{2}g_0(\bar{\psi}\gamma_\mu\psi)^2 \quad (2.1)$$

The massless model ($m_0=0$) was proposed by Thirring¹⁰ in 1958 as an example of a nontrivial relativistic fermionic field theory. There is a vast literature analyzing the massless case,¹¹ and more recently the full structure of the massive model was exposed.⁵ The massive model possesses a rich spectrum, which makes it an interesting toy model for Monte Carlo studies. For couplings $g_0 > 0$, the particle content consists of fermions and one or more bound states. The number of bound states is determined by the strength of the coupling. Since the spectrum of this model is known exactly for the case of infinite volume, it is a natural candidate for an analysis of finite volume effects in Monte Carlo calculations. The presence of both fermions and bosons in the spectrum will allow us to determine how the fermionic and bosonic sectors of a field theory respond to volume and boundary effects.

A direct latticization of the massive Thirring model action is possible using either the Wilson or Kogut-Susskind formulation of lattice fermions. However, either of these approaches would introduce the standard problems associated with Monte Carlo simulation of fermions. Alternatively, one might introduce the sine-Gordon boson field on the lattice. The implementation of a Monte Carlo algorithm would be straightforward in the bosonic formulation, but such an

approach would make it difficult to study some of the quantities we wish to calculate such as fermion correlation functions and fermion-antifermion bound state wave functions. Thus we will eschew the conventional procedures for putting the massive Thirring/sine-Gordon model on a lattice and instead take advantage of the connection between fermion models and spin systems which exists in two dimensions. This relation was discovered long ago by Jordan and Wigner,¹² who explicitly wrote down the transformation from a spin operator to a fermion operator. It is an essential feature of the Onsager-Kaufmann¹³ treatment of the two-dimensional Ising model. In that case the Jordan-Wigner transformation reduces the model to a system of free fermions, as discussed in detail by Schultz, Mattis, and Lieb.¹⁴ The Baxter model may be thought of as a staggered pair of Ising lattices with four-spin couplings in addition to the nearest neighbor Ising couplings. By exploiting the connection between the Baxter lattice and the XYZ Heisenberg spin chain Hamiltonian,¹⁵ Luther⁴ showed that, just as in the Ising case, the Baxter model could be transformed to a fermion theory via a Jordan-Wigner transformation. The four-spin interaction leads to a Thirring four-fermion interaction, and in the scaling limit the theory reduces to the massive Thirring model. The Baxter model is therefore an acceptable latticization of the massive Thirring model. Furthermore, since the Baxter model is solvable, we have analytic expressions for the spectrum of the massive Thirring model on a lattice. Thus, there is no need to take the $a \rightarrow 0$ limit in order to separate finite volume effects in the calculations.

The action for the Baxter model on a lattice of M rows and N columns is given by

$$S = - \sum_{i=1}^M \sum_{j=1}^N [J \sigma_{i,j+1}^z \sigma_{i+1,j}^z + J' \sigma_{ij}^z \sigma_{i+1,j+1}^z + J_4 \sigma_{ij}^z \sigma_{i,j+1}^z \sigma_{i+1,j}^z \sigma_{i+1,j+1}^z]. \quad (2.2)$$

Here we are using the spin formulation of the model. An equivalent "arrow" formulation reveals the Baxter model as a generalized ice-type model with eight distinct vertices (c.f. Ref. 3, Appendix A). There are four independent vertex weights a , b , c , and d , whose relation to J , J' , and J_4 is given in (3.12). The overall scale of the vertex weights enters trivially and there are thus three nontrivial parameters which determine the vertex weights. It is convenient to introduce Baxter's elliptic function parametrization of these weights and define the parameters v and η and the elliptic modulus k by

$$a:b:c:d = \text{sn}(v+\eta|k):\text{sn}(v-\eta|k):\text{sn}(2\eta|k):k\text{sn}(v+\eta|k)\text{sn}(v-\eta|k)\text{sn}(2\eta|k) \quad (2.3)$$

where $\text{sn}(x|k)$ is a Jacobian elliptic function of argument x and modulus k . This parametrization of the vertex weights has the important feature that all transfer matrices having the same value of k and η , but arbitrary values of v , will commute with each other. Thus the transfer matrices $T(v)$ for all v are simultaneously diagonalized by a set of eigenvectors which are independent of v .

We now briefly review the relation between the Baxter model and the massive Thirring model.⁴ The connection is established in two steps. The first step relates the Baxter and XYZ spin chain models. The XYZ spin chain is described by the Hamiltonian

$$H_{XYZ} = -\frac{1}{2} \sum_{n=1}^N (J_x \sigma_n^1 \sigma_{n+1}^1 + J_y \sigma_n^2 \sigma_{n+1}^2 + J_z \sigma_n^3 \sigma_{n+1}^3) , \quad (2.4)$$

with $\sigma_{N+1}^i = \sigma_1^i$. The relation between the Baxter model transfer matrix $T(v)$ and the Hamiltonian H_{XYZ} was demonstrated by Baxter,¹⁵ who proved that H_{XYZ} is essentially the logarithmic derivative of $T(v)$ with respect to v . Indeed, he showed that if the couplings J_x, J_y , and J_z are parametrized as

$$J_x : J_y : J_z = \text{cn}(2\xi|1) : \text{dn}(2\xi|1) : 1 \quad (2.5)$$

where $\xi = -i(1+k)\eta$ and $l = (1-k)/(1+k)$, then the Hamiltonian, Eq.(2.4) is obtained from the Baxter model transfer matrix T by the formula

$$H_{XYZ} = -J_z \text{sn}(2\xi|1) \times \left. \frac{d}{dV} \log T(V) \right|_{V=\xi} - \frac{N}{2} [\text{cn}(2\xi|1) + \text{dn}(2\xi|1) - 1] / \text{sn}(2\xi|1) \quad (2.6)$$

where $V = -i(1+k)v$. Since T and H_{XYZ} commute, both operators have identical eigenvectors, and the eigenvalues of these two operators are also related by (2.6). The second step makes use of the Jordan-Wigner transformation to map the XYZ Hamiltonian onto a lattice massive Thirring model. The Jordan-Wigner transformation maps the Pauli spin operators onto a set of fermionic operators, c_n . If

$$c_n = \prod_{j=1}^{n-1} \exp(i\pi \sigma_j^+ \sigma_j^-) \sigma_n^- , \quad (2.7)$$

$$c_n^\dagger = \sigma_n^+ \prod_{j=1}^{n-1} \exp(-i\pi \sigma_j^+ \sigma_j^-) ,$$

where $\sigma^\pm = \frac{1}{2}(\sigma^1 \pm i\sigma^2)$, then $\{c_n, c_m^\dagger\} = \delta_{n,m}$ and $\{c_n, c_m\} = 0$. The Hamiltonian, Eq.(2.4), when expressed in terms of the c_n , assumes the form

$$H_{XYZ} = -\frac{1}{2} \sum_{j=1}^N \left\{ i(J_x + J_y) [c_j^\dagger c_{j+1} + c_j c_{j+1}^\dagger] - i(-)^j (J_x - J_y) [c_j^\dagger c_{j+1}^\dagger + c_j c_{j+1}] \right. \\ \left. + 4J_z [c_j^\dagger c_j - \frac{1}{2}] [c_{j+1}^\dagger c_{j+1} - \frac{1}{2}] \right\} , \quad (2.8)$$

where the further transformation $c_n \rightarrow (i)^n c_n$, has been applied. In the Dirac representation (γ^0 diagonal), one defines the two-component Thirring field ψ by identifying the upper component ψ_1 with c_j for even j and the lower component ψ_2 with the c_j for odd j (staggered fermions):

$$\psi = \begin{pmatrix} \psi_1 \\ \psi_2 \end{pmatrix} \quad (2.9)$$

The field equations for ψ are obtained via the Heisenberg equations of motion

$$\dot{\psi}_\alpha = i[H_{XYZ}, \psi_\alpha] , \quad \alpha=1,2 \quad (2.10)$$

which yield the equations of motion for the Thirring model when the lattice spacing is taken to zero.

III. Exact Expressions for the Fermion and Bound State Masses

Masses are obtained by evaluating two-point functions

$$\Delta(x, \tau) = \langle 0 | \theta(x, \tau) \theta(0) | 0 \rangle \quad (3.1)$$

of operators θ carrying the quantum numbers of the particle whose mass one wants to determine. The effect of integrating $\Delta(x, \tau)$ over the spatial direction is to project out those states with zero momentum, and thus the mass m of the lowest excitation in a particular channel can be read off from the large τ behavior (where τ is Euclidean time):

$$\tilde{\Delta}(\tau) = \int d^3x \Delta(x, \tau) \sim Z e^{-m\tau} \quad \text{for } \tau \rightarrow \infty \quad (3.2)$$

where Z is a renormalization constant. For field theory on a lattice, the integral is replaced by a sum over spatial lattice sites.

In this work, we are interested in analyzing finite volume effects in the Monte Carlo calculation of the massive Thirring model spectrum, so we seek operators carrying the quantum numbers of the fermion and lowest mass bound state, respectively. In the Ising spin language, the Thirring fermion mass m_F may be extracted from the spin-spin correlation function when $T > T_c$,

$$\tilde{F}(\tau) = \sum_x \langle \sigma_{0,0} \sigma_{x,\tau} \rangle \sim Z_F e^{-m_F \tau} \quad , \quad (3.3)$$

while the bound state mass m_B is obtained from the correlation function between composite operators θ constructed from the product of adjacent spins, i.e.

$$\tilde{B}(\tau) = \sum_x \langle \sigma_{0,0}^0 \sigma_{0,1}^0 \sigma_{x,\tau}^0 \sigma_{x,\tau+1}^0 \rangle - Z_B e^{-m_B \tau} \quad (3.4)$$

On a periodic lattice, the masses are extracted by fitting the Monte Carlo data to the expressions

$$\tilde{F}(\tau) = Z_F (e^{-m_F \tau} + e^{-m_F (N-\tau)}) \quad (3.5)$$

$$\tilde{B}(\tau) = Z_B (e^{-m_B \tau} + e^{-m_B (N-\tau)}) \quad (3.6)$$

where N is the extent of the lattice in the τ -direction, and Z_F and Z_B are the fermion and bound state wavefunction renormalization constants, respectively.

The fermion and boson masses m_F and m_B may be exactly calculated on an infinite volume lattice with arbitrary lattice spacing a . The results of these calculations, expressed in terms of Baxter's parametrization are

$$m_F a = -\frac{1}{2} \log k_2 \quad , \quad (3.7a)$$

$$m_B a = -\log \left[k_2 / \operatorname{dn}^2 \left[\left(\frac{K_2}{\pi} \right) (\tau(\mu) - 2\lambda), k_2 \right] \right] \quad , \quad (\pi/2 \leq \mu \leq \pi) \quad (3.7b)$$

where k_2 is the modulus of the complete elliptic integral K_2 defined by

$$\pi K_2' / K_2 = 2\lambda \quad , \quad (3.8)$$

and

$$\lambda = -i\pi\eta/K_k \quad (3.9)$$

where η and k are the parameters defined in (2.3). In these expressions dn is a Jacobian elliptic function, and K_2' and K_k are the complete elliptic integrals of modulus $k_2'=(1-k_2^2)^{1/2}$ and k , respectively. The parameter μ is given by

$$\mu = \frac{\lambda K_1'}{K_1} \quad (3.10)$$

where $l=(1-k)/(1+k)$ and $l'=(1-l^2)^{1/2}$. The relation between μ and the coupling g_0 of the continuum theory is

$$\cot \mu = -g_0/2 \quad (3.11)$$

The interval $0 < \mu < \pi$ covers the range $-\infty < g_0 < \infty$. Free field theory obtains when $\mu = \pi/2$. The bound state spectrum appears for $\mu > \pi/2$ with a new bound state appearing in the spectrum each time a point $\mu = \pi - \pi/n$ ($n=2,3,4,\dots$) is crossed. The modulus k_2 completely specifies the fermion mass, via Eq.(3.7a). The bound state mass is given in terms of k_2 and μ , via Eq.(3.7b).

In order to carry out the simulations on the Baxter model expressed in the spin language, Eq.(2.2), we need to relate the spin couplings J , J' , and J_μ , to the vertex weight functions a,b,c,d . The needed relations are

$$\beta J = \frac{1}{4} \log(ad/bc) \quad (3.12a)$$

$$\beta J' = \frac{1}{4} \log(ac/bd) \quad (3.12b)$$

$$\beta J_{\mu} = \frac{1}{4} \log(ab/cd) \quad (3.12c)$$

where the vertex weights are specified in Eq.(2.3). In selecting the parameters for the Monte Carlo simulations, we first select k_2 and μ in order to fix the masses of the fermion and bound states. Corresponding values for η and k result via the relations (3.8)-(3.10). In order to work with isotropic lattices, we have set $v=0$ throughout the calculations. This allows a unique determination of the weights a , b , c , and d which are then translated into the spin couplings J , J' , and J_{μ} using (3.12).

IV. Monte Carlo Calculations

Our first analysis deals with the effect of finite volume on the Monte Carlo calculation of the mass of the Thirring fermion in the free field case ($\mu=\pi/2$). On the lattice, this limit is realized in the form of two independent (decoupled) nearest neighbor Ising lattices. We first carried out a preliminary calculation of the spontaneous magnetization, as a check of our Monte Carlo algorithm, and for a rough indication of the kind of statistics we might anticipate. The spontaneous magnetization M is taken to be

$$M = \langle \sum_k \sigma_k \rangle / V \quad (4.1)$$

where the sum runs over all lattice sites, V is the lattice volume, and the angular brackets denote an ensemble average. Strictly speaking, M should be defined by applying a small uniform magnetic field, taking the infinite volume limit, and then letting the field go to zero, since, for zero field and finite volume there is a nonvanishing probability of tunneling from positive to negative magnetization. However, for the size lattices we are using this tunneling probability is negligible even for temperatures quite close to critical, and M may be calculated from (4.1) using an ensemble generated with zero field from a "cold start," $\sigma_i=+1$ for all spins i , or from a "hot start" (random spins), by considering only the absolute value of M in each Monte Carlo run. For the two-dimensional Ising model, the exact form of M is given by

$$M = [1 - (\sinh(2\beta J_1)\sinh(2\beta J_2))^{-2}]^{1/8} , \quad (4.2)$$

where the J_i are the couplings in the two orthogonal directions. For our calculation of M , we performed a Monte Carlo simulation on a 30×30 isotropic ($J_1=J_2=1$) lattice for $\beta=.20,.30,.40,.42,.45,.50,.60,.70$, and $.80$. The critical temperature is given by $\sinh 2\beta_c=1$, or $\beta_c=.44068\dots$ For each β value, we initialized with a hot start and let the system come to equilibrium by sweeping through the lattice 1000 times. After that, a configuration was saved every 50 sweeps. The results for the magnetization shown in Fig. 1 are based on ensembles of 1000 configurations for each β value. A study of subensembles revealed no significant correlation between configurations separated by 50 sweeps, and the error bars shown in Fig. 1 are purely statistical.

Our calculation of the fermion mass in the Ising (free fermion) case was carried out on 8×30 , 10×30 , 12×30 , 14×30 , 20×30 , and 30×30 lattices for $k_2=.7902$, corresponding to a mass $m_F a=.1178$ in the infinite volume limit. As in the magnetization calculation, the simulation was initiated with a hot start, and after equilibrating for 1000 sweeps, a configuration was saved after every 50 sweeps. For each lattice, a total of 6000 configurations were saved (corresponding to a total of 300,000 sweeps). This required a total of about two hours of CPU time on a Cyber 175 or about 12 hours on a VAX 11/780. The extraction of the fermion mass follows from computing the spin-spin correlation function Eq. (3.3) averaged over the ensemble and then fitting the results to the exponential form in Eq. (3.5). In all cases the correlation function fit extremely well to a pure exponential over a large number of data points. Fig. 2 shows a typical set of results for the spin-spin

correlation on a 30×30 lattice together with the exponential fit. Statistical errors on the fermion mass were computed by dividing the full set of 6000 configurations into various subensembles. The results for the mass as a function of lattice volume are shown in Fig. 3. The dashed line is the theoretical infinite volume result. It should be noted that, for a one-fermion state (or more generally for a state with an odd number of fermions), the imposition of periodic boundary conditions on the spin system corresponds to non-periodic boundary conditions on the fermions. This gives rise to nonvanishing finite volume effects even in the free fermion case. This subtlety does not arise in the calculation of boson masses, which will be the main focus of this paper. We note that the mass $m_{F,a} = .1178$ corresponds to a fermion Compton wavelength of about $8\frac{1}{2}$ sites. The results shown in Fig. 3 confirm the expectation that finite size effects become appreciable when the lattice size is comparable to or smaller than twice the Compton wavelength (the factor of two coming from the periodicity of the lattice).

We next investigate the volume effects in the full, interacting theory. With the two parameters k_2 and μ at our disposal, we are free to adjust the fermion and bound state masses independently of each other. Calculations were performed on 6×30 , 10×30 , 20×30 , 30×30 , 50×50 , and 100×100 lattices with $k_2 = .7902$ and $\mu = .65\pi$, on 10×30 , 20×30 , 30×30 , and 50×50 lattices with $k_2 = .7250$ and $\mu = .73\pi$, on 10×30 , 20×30 , and 30×30 lattices with $k_2 = .6645$ and $\mu = .65\pi$, and on a 30×30 lattice with $k_2 = .4212$ and $\mu = .82\pi$. A total of 6000 configurations for each choice of parameters and lattice size were generated in the manner already described. The calculation of fermion and boson masses is obtained from the asymptotic

behavior of the correlation functions (3.3) and (3.4) respectively. In both cases, the correlation functions fit extremely well to an exponential over a large range of points, and the mass values could be extracted with very good accuracy. A typical boson correlation function on a 30×30 lattice is shown in Fig. 4.

For the first set of calculations, we kept k_2 fixed at the value which was used for the free fermion case ($k_2 = .7902$), so that we could directly compare the behavior of the fermion mass calculations for two different couplings μ , i.e. $\mu = \pi/2$ and $\mu = .65\pi$. The exact, infinite volume values for the fermion and bound state masses for $k_2 = .7902$ and $\mu = .65\pi$ are $m_{Fa} = .1178$ and $m_{Ba} = .1762$. The results of the mass calculations for this parameter choice are presented in Fig. 5. The response of the fermion mass to shrinking the lattice from 100×100 down to 30×30 is minimal, as we might have anticipated from the results in the decoupling limit. There is a slight dip in the mass for the 20×30 lattice. This is distinct from the result for the same lattice size in the free fermion case, where the fermion mass undergoes a 6% upward shift from its infinite volume value. An even more noticeable distinction between the free field and interacting theories occurs at the 10×30 lattice. In the free field calculation, the mass suffers a 27% upward shift, while for the $\mu = .65\pi$ case, the shift is only 15%.

Of greater interest is the striking behavior of the bound state mass. We find that this mass decreases substantially from its infinite volume value,¹⁷ reaches a minimum, and then eventually increases to pass above the infinite volume value as the lattice is taken to very small sizes. This dramatic response to varying the size of the lattice is actually the result of two competing effects. The first effect,

responsible for the decrease in mass, is associated with the extended size of the bound state. We can understand this effect by appealing to a simple potential model description for the bound state. Let $V_\infty(x) < 0$ be the potential in an infinite volume responsible for binding the Thirring fermions into a bound state, and let ΔE_∞ denote the corresponding binding energy. By putting the system on a finite lattice with spatial extent L , and periodic boundary conditions, the actual potential is no longer given by V_∞ , but is instead

$$V_L(x) = \dots + V_\infty(x-2L) + V_\infty(x-L) + V_\infty(x) + V_\infty(x+L) + V_\infty(x+2L) + \dots \quad (4.3)$$

and in particular, $V_L(x) < V_\infty(x)$. The effective finite lattice potential, V_L , provides a deeper well, for a given x , than does the infinite lattice potential V_∞ . This leads to an increase in the binding energy $\Delta E_L > \Delta E_\infty$. Since the bound state mass is given by $m_B = 2m_F - \Delta E$, for fixed or slowly varying values of m_F , we expect $(m_B)_L < (m_B)_\infty$. The second effect, which is responsible for the increase of the bound state mass for very small lattices, is due to the finite size effects suffered by the constituent fermions themselves. We have seen how the fermions respond when the lattice is varied to sufficiently small sizes. For such lattice sizes, m_F is increasing rapidly and supplies a positive contribution to m_B . Since both these effects are present, they combine to lead to the observed response of the bound state mass to variation of the lattice volume.

Based on the above description, if the fermion were to suffer no finite size effects, we would expect the bound state mass to monotonically decrease from its infinite volume value as the lattice

volume is decreased. We confirmed this expectation by performing a second set of calculations, with appropriate changes in the parameters. We kept $\mu=.65\pi$ and adjusted $k_2=.6645$, thereby increasing the fermion mass (decreasing its Compton wavelength) to $m_{F,a}=.2043$. The fermion should now be fairly immune to finite size effects over a wide range of lattice sizes. The new bound state mass is $m_{B,a}=.3054$. The calculated masses are shown in Fig. 6. The fermion mass is indeed unaffected, even for lattices as small as 10×30 . The bound state mass, in marked contrast, decreases monotonically with diminishing lattice volume.

Another set of bound state mass calculations which complements these considerations is shown in Fig. 7. For this set, $k_2=.7250$ and $\mu=.73\pi$, which yields $m_{B,a}=.1762$ and $m_{F,a}=.1608$. The bound state mass suffers a slightly smaller shift from its infinite volume limit as compared to the results in Fig. 5. The difference is that the coupling μ is stronger, and hence the bound state wavefunction is less spread out, as we will now demonstrate.

The above argument that the bound state mass is expected to decrease as the lattice size becomes smaller due to the fact that the potential is lowered by the periodic contributions in (4.3) also implies that the size lattices for which this effect becomes important is determined by the size of the bound state. We may confirm this interpretation of the finite size effects by directly studying the bound state wavefunction on the lattice. The wavefunction may be obtained from the same Monte Carlo data used for the spectral calculations. Recall that the boson mass was obtained from the correlation function for the operator $\Theta(i,\tau)=\sigma_{\tau,i}\sigma_{\tau,i+1}$ on two different time slices τ . To obtain the bound state wavefunction, we consider the correlation

function between this operator and a spread out operator $\Theta(i, \tau; x) = \sigma_{\tau, i}^0 \sigma_{\tau, i+x}^0$. The bound state wavefunction $\psi(x)$ is then obtained from the large τ behavior of this correlation function, i.e.

$$\tilde{B}(x, \tau) = \sum_y \langle \sigma_{0,0}^0 \sigma_{0,1}^0 \sigma_{\tau,y}^0 \sigma_{\tau,y+x}^0 \rangle \sim \psi(x) e^{-m_B \tau} \quad \text{for } x \text{ odd} \quad (4.4)$$

In the nonrelativistic limit of the continuum theory, the function $\psi(x)$ reduces to the Schrodinger bound state wavefunction. More generally, we expect this function to give a reliable indication of the size of the bound state. The calculation was done on a 30×30 lattice for $\mu = .65\pi$ and $k_2 = .7902$, for $\mu = .73\pi$ and $k_2 = .7251$, and for $\mu = .82\pi$ and $k_2 = .4212$. Since the Monte Carlo configurations had already been generated for the spectral analysis, the calculation of wavefunctions required only an additional two to three minutes of Cyber 175 time for each choice of parameters. The theoretical infinite volume value of the bound state mass for each of these three cases was fixed to be $m_B a = .1762$. The masses calculated from the Monte Carlo data were $m_B a = .1348 \pm .0024$, $.1548 \pm .0042$, and $.1751 \pm .0050$, for $\mu = .65\pi$, $.73\pi$, and $.82\pi$ respectively. The corresponding wavefunctions, $|\psi(x)|^2$, are plotted in Fig. 8. We see clearly that the deviation of the bound state mass from its infinite volume value is directly correlated with the relative size of the lattice and the bound state. For the strongest of the three couplings ($\mu = .82\pi$) the wavefunction is essentially completely contained within the volume of the lattice ($|\psi(15)|^2 / |\psi(1)|^2 = .005$) and correspondingly, the measured mass is essentially equal to the infinite volume value ($.1751 \pm .0050$ compared to $.1762$). From this same perspective, we can also understand the previous results obtained from varying the lattice

size for fixed coupling. For example, at $\mu=.65\pi$, the measured bound state mass was $m_B=.1330\pm.0021$, $.1673\pm.0052$, and $.1808\pm.0046$ for lattices of spatial size $L=30$, 50 , and 100 sites respectively (c.f. Fig. 5), to be compared with the infinite volume value $.1762$. The corresponding bound state wavefunctions at maximum separation N on each lattice give $|\psi(N)|^2/|\psi(1)|^2=.403$, $.105$, and $.0027$ for $N=15$, 25 , and 49 respectively. Again we see that the infinite volume result for the bound state mass is obtained when the lattice is large enough to completely contain the bound state wavefunction.

V. Conclusions and Discussion

We have taken advantage of the exact solvability of both the massive Thirring model and its discrete lattice counterpart, the Baxter model, to make a precise determination of the magnitude and nature of finite lattice volume effects in Monte Carlo mass calculations. Our results show clear evidence for substantial finite volume effects, and we have found definite criteria for what is meant by a "small" lattice. In the case of an "elementary" particle (i.e. the fermion in the weakly coupled Thirring model), the relevant size scale is set by twice the Compton wavelength of the particle. The measured mass of this particle is substantially shifted from its infinite volume value when the lattice size is comparable to or smaller than this scale. In the Baxter/Thirring model, the finite size effects tend to increase the mass of the fermion. For the calculation of the fermion-antifermion bound state masses, the relevant length scale is determined not by the Compton wavelength (i.e. inverse mass) of the bound state, but by the spatial extent of the wavefunction. In this case, a small lattice is one with a spatial size smaller than the spread of the bound state wavefunction. This was convincingly demonstrated by varying both the lattice size and the bound state size.

Although our results have been obtained in a simple toy model, we expect that much of what we have found will have implications for Monte Carlo studies of realistic field theories such as QCD. There have been some recent Monte Carlo results for hadron wave functions.¹⁸ Such calculations should give a clear indication of the importance of finite size effects on the spectrum. If these effects are nonnegligible, it

may be possible to obtain a quantitative estimate of them using the information provided by the wavefunction on a fixed size lattice.

Acknowledgements

One of us (DH) would like to thank his thesis advisor Prof. C. Quigg for his patience, support, and enthusiasm while this work was in progress. One of us (HBT) would like to thank the Aspen Center for Physics where some of this work was carried out. We are grateful to W. A. Bardeen for useful discussions. We would also like to thank the Fermilab Computer Department for the use of its facilities.

References

1. See for example, Gauge Theory on a Lattice:1984 , Proceedings of the Argonne National Laboratory Workshop, C. Zachos et al, eds., Conf-8404119
2. P. Hasenfratz and I. Montvay, Phys. Rev. Lett. 50, 309 (1983).
3. R. J. Baxter, Ann. Phys. (N.Y.) 70, 193 (1972).
4. A. Luther, Phys. Rev. B14, 2153 (1976).
5. H. Bergknoff and H. B. Thacker, Phys. Rev. D19, 3666 (1979).
6. J. D. Johnson, S. Krinsky, and B. M. McCoy, Phys. Rev. A8, 2526 (1973).
7. S. Coleman, Phys. Rev. D11, 2088 (1975).
8. R. Dashen, B. Hasslacher, and A. Neveu, Phys. Rev. D11, 3424 (1975).
9. Our notation for the Baxter parameters follows the conventions of Refs. 3 and 6.
10. W. Thirring, Ann. Phys. 3, 91 (1958).
11. For a definitive treatment of the massless model, see B. Klaiber, in Lectures in Theoretical Physics , lectures delivered at the Summer Institute for Theoretical Physics, University of Colorado, Boulder, 1967, edited by A. Barut and W. B. Brittin (Gordon and Breach, New York, 1968), Vol. X, part A.
12. P. Jordan and E. Wigner, Z. Physik 47, 631 (1928).
13. L. Onsager, Phys. Rev. 65, 117 (1944); B. Kaufman, Phys. Rev. 76, 1232 (1949); B. Kaufman and L. Onsager, Phys. Rev. 76, 1244 (1949).

14. T. D. Schultz, D. C. Mattis, and E. H. Lieb, Rev. Mod. Phys. 36, 856 (1964).
15. R. J. Baxter, Ann. Phys. (N.Y.) 70, 323 (1972).
16. E. H. Lieb, T. D. Schultz, and D. C. Mattis, Ann. Phys. (N.Y.) 16, 407 (1961).
17. A qualitatively similar behavior in lattice QCD has been suggested on the basis of analytic arguments (K. Olynyk, private communication).
18. D. Weingarten and B. Velikson, Preprint 84-0727 (IBM).

Figure Captions

1. Spontaneous magnetization of the Ising model as a function of inverse temperature.
2. Spin-spin correlation function, Eq. (3.3), on a 30×30 lattice for weakly attractive coupling ($\mu = .65\pi$).
3. Fermion mass as a function of spatial lattice volume for noninteracting fermions ($\mu = .50\pi$).
4. Boson correlation function, Eq. (3.4), on a 30×30 lattice for weakly attractive coupling ($\mu = .65\pi$).
5. Fermion and bound state masses as a function of lattice volume for weakly attractive coupling ($\mu = .65\pi$).
6. Fermion and bound state masses as a function of lattice volume for weakly attractive coupling ($\mu = .65\pi$) with a heavier fermion.
7. Bound state mass as a function of lattice volume for stronger coupling ($\mu = .73\pi$).
8. Bound state wave function, defined in Eq. (4.4), for three values of coupling strength.

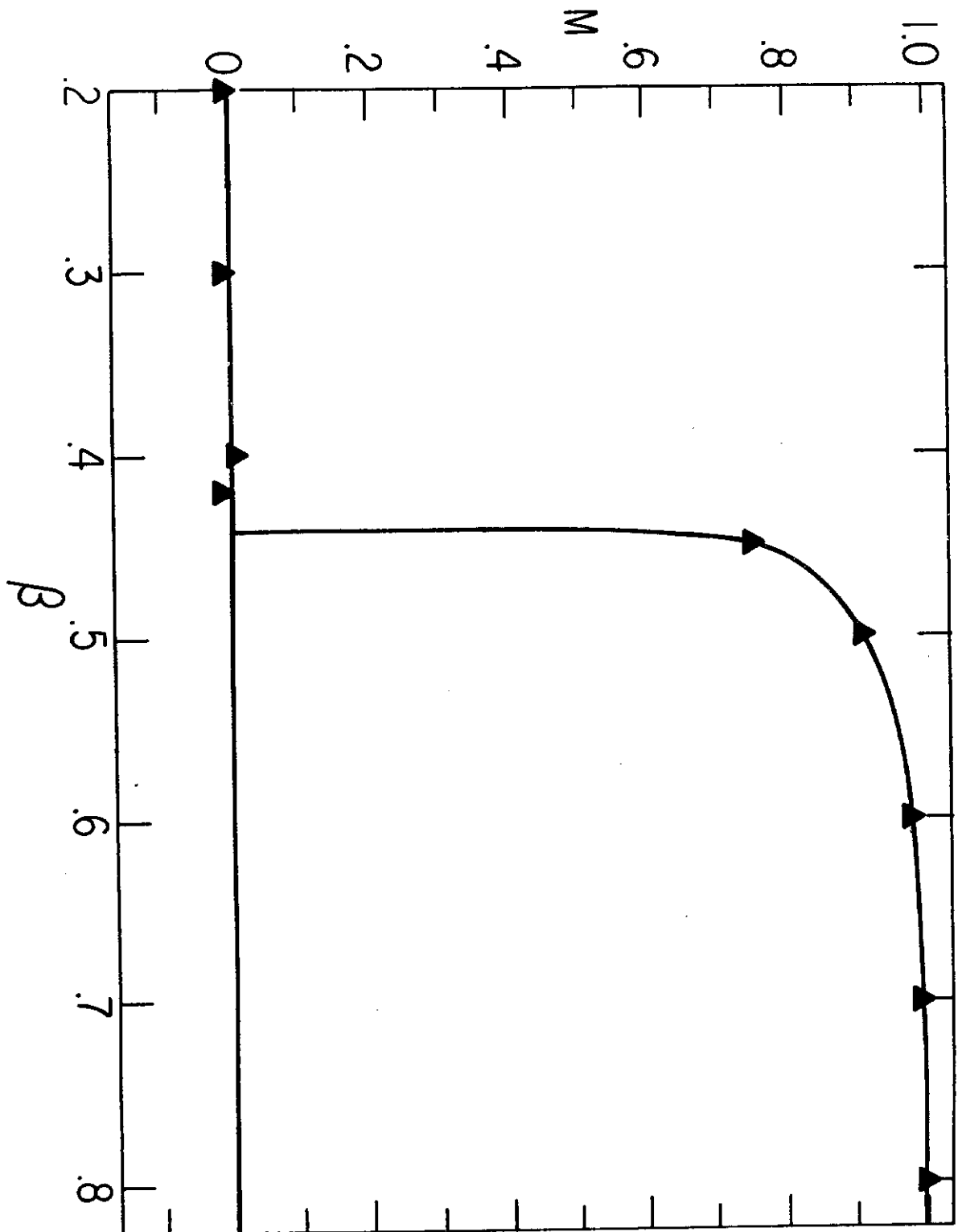


Fig. 1

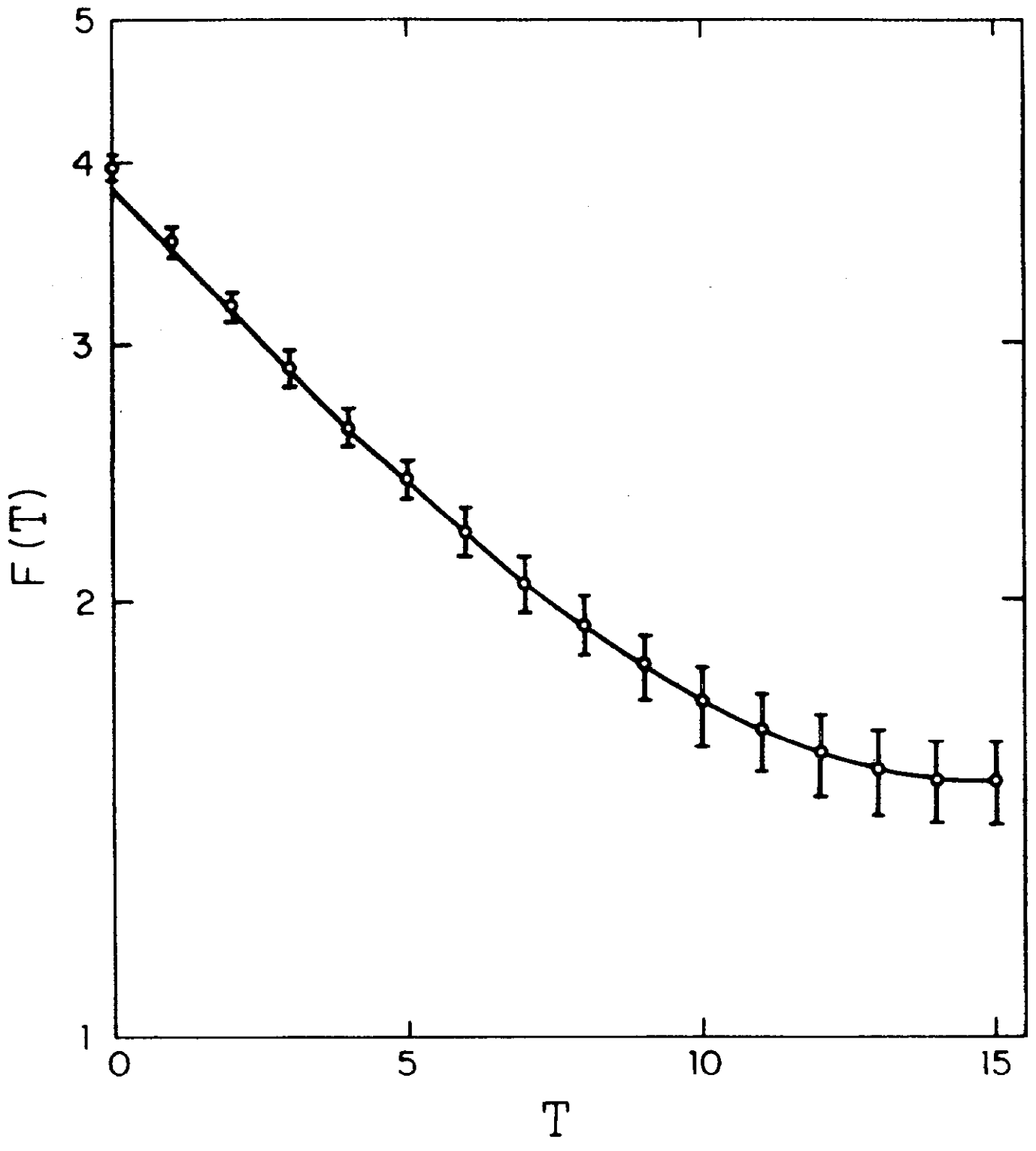


Fig. 2

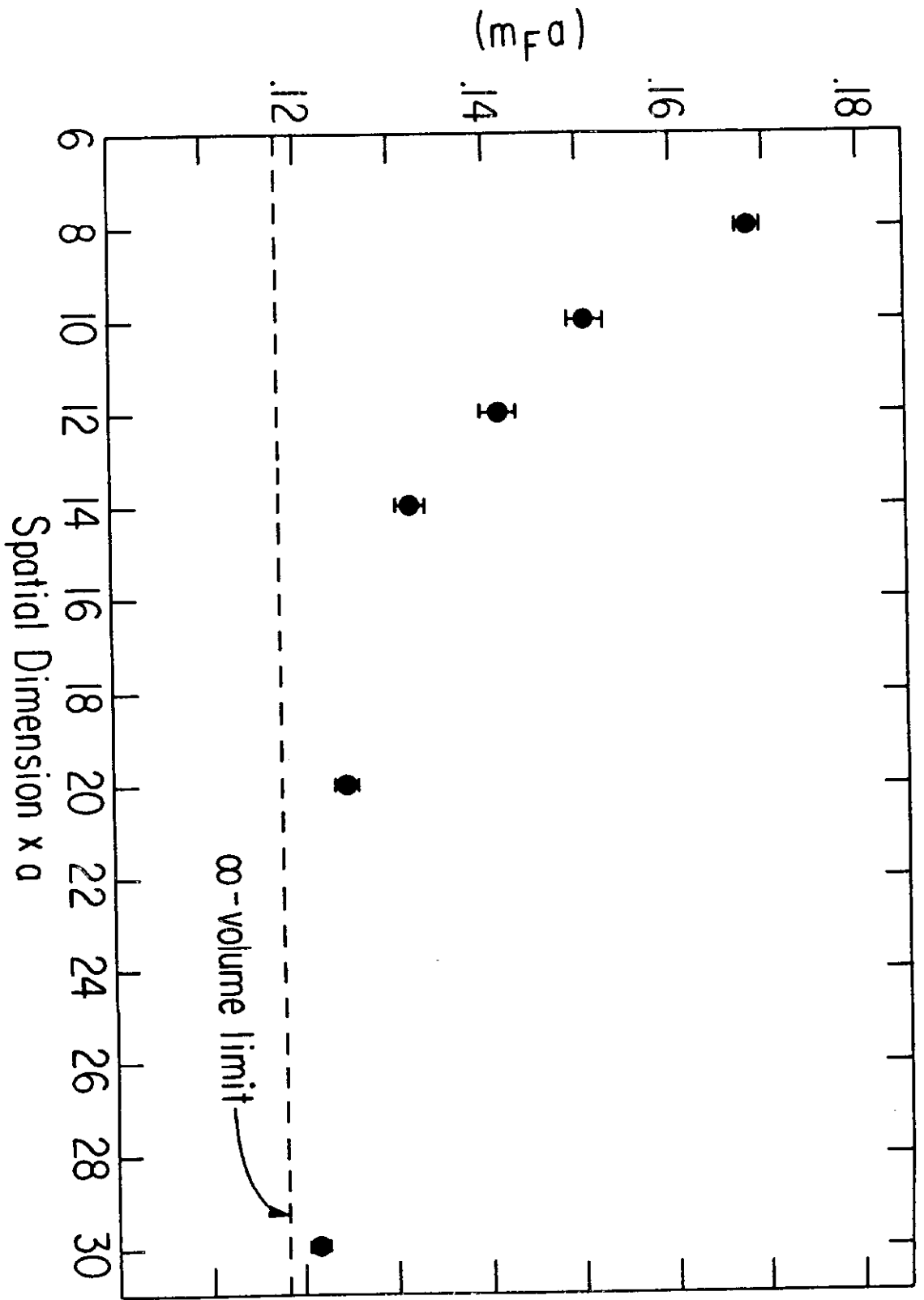


Fig. 3

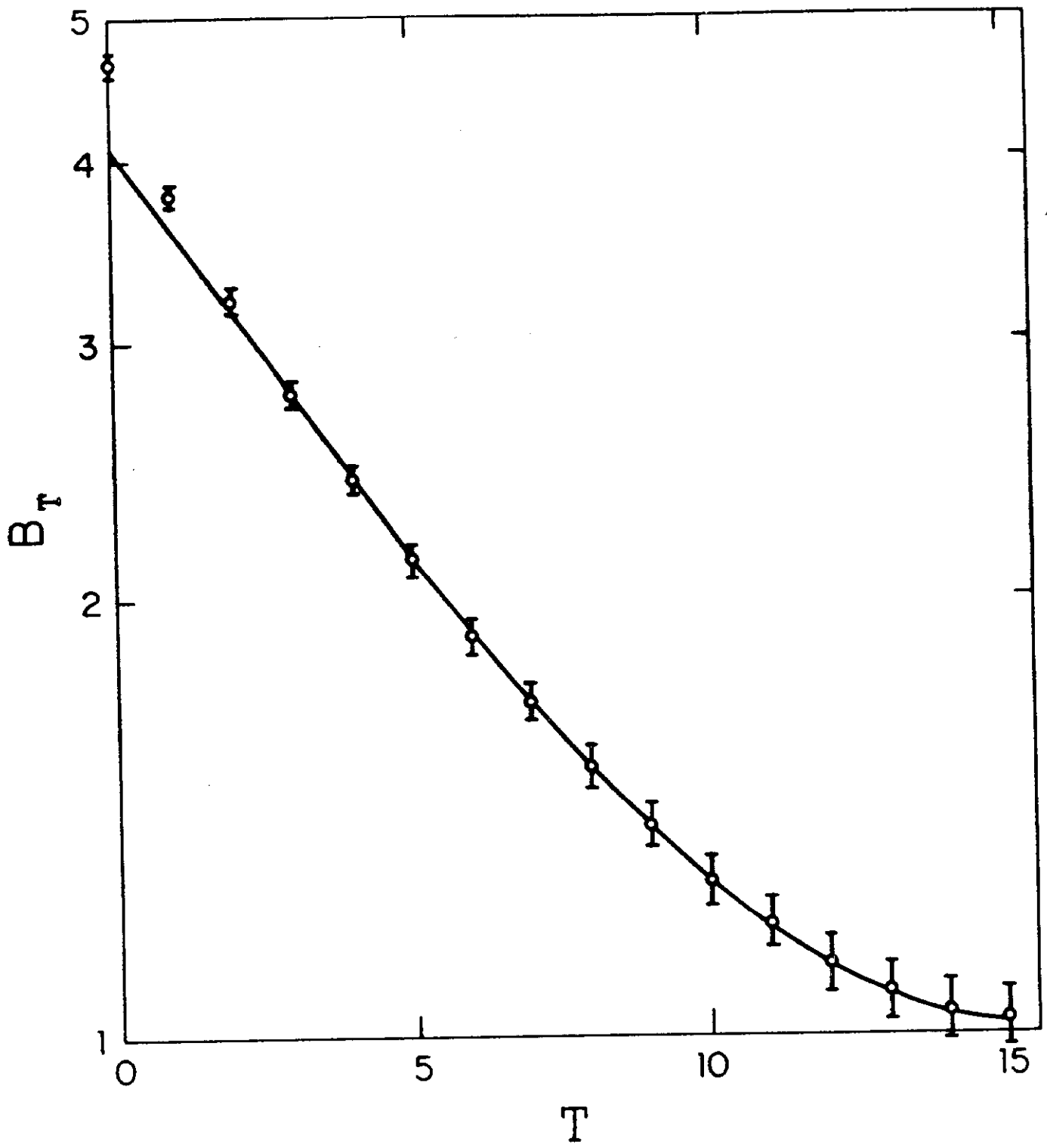


Fig. 4

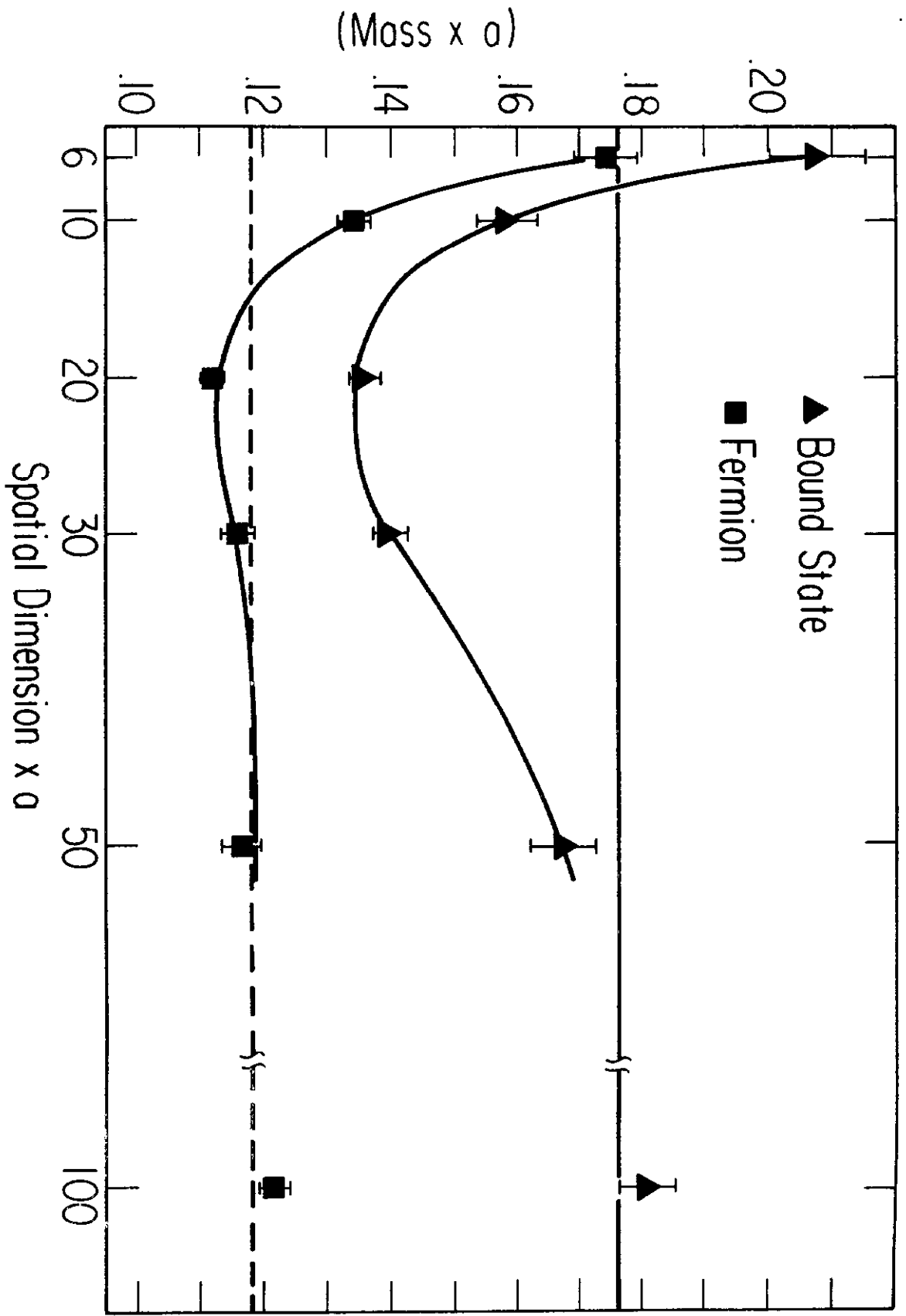


Fig. 5

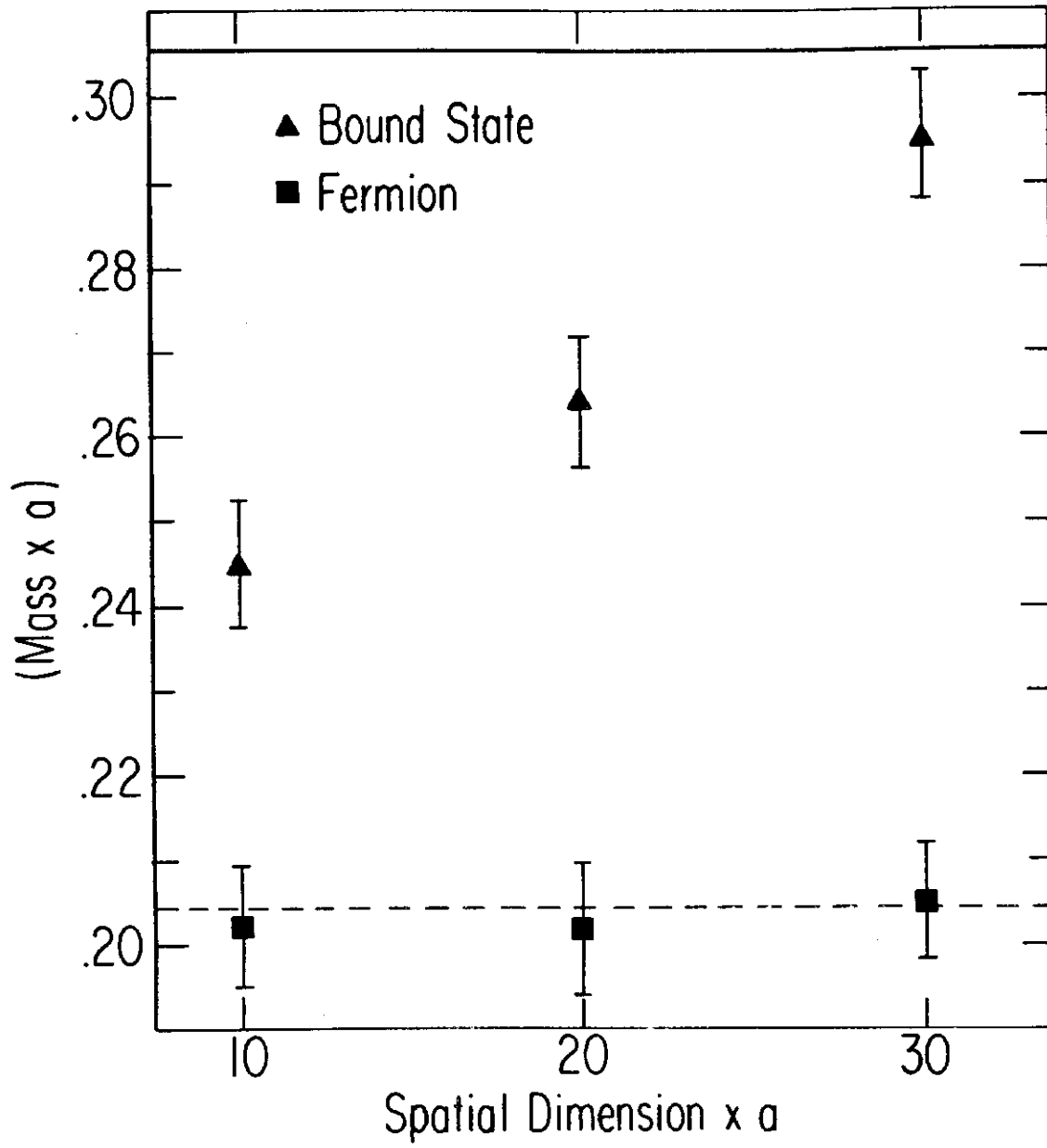


Fig. 6

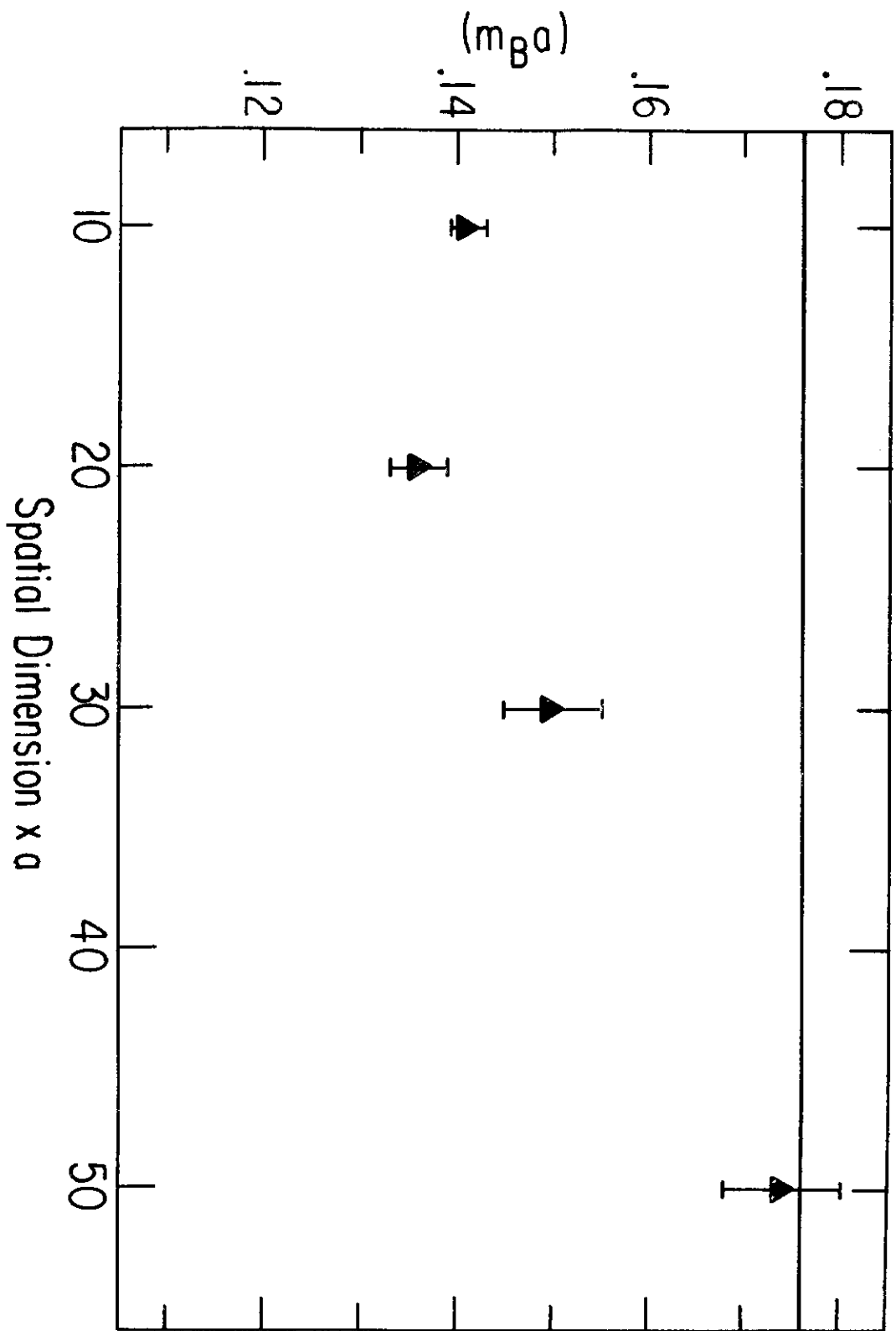


Fig. 7

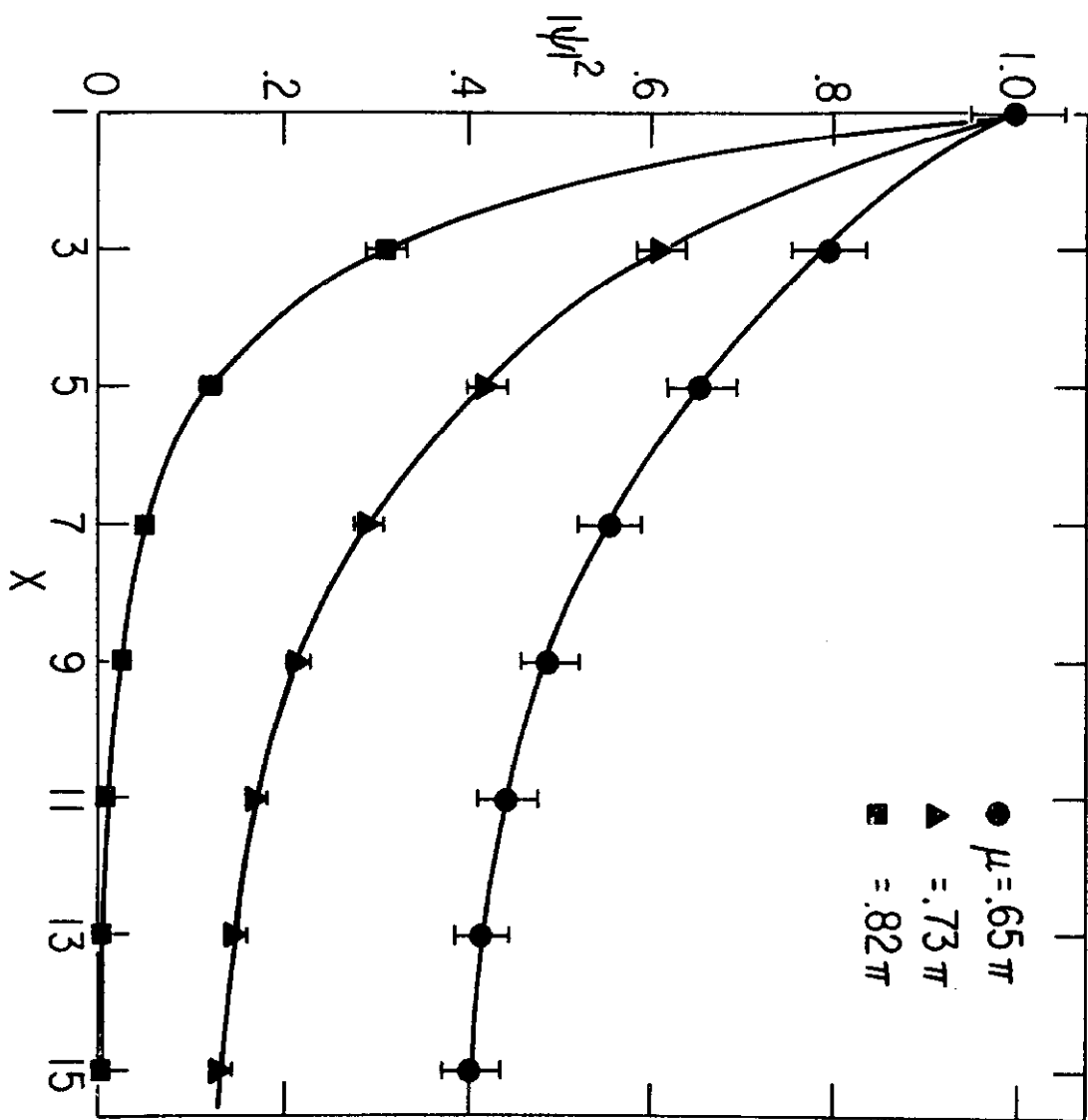


Fig. 8